Technical Note

Physiorack: An Integrated MRI Safe/Conditional, Gas Delivery, Respiratory Gating, and Subject Monitoring Solution for Structural and Functional Assessments of Pulmonary Function

Ahmed F. Halaweish, PhD,[1,2] and H. Cecil Charles, PhD[1,2]*

Purpose: To evaluate the use of a modular MRI conditional respiratory monitoring and gating solution, designed to facilitate proper monitoring of subjects' vital signals and their respiratory efforts, during free-breathing and breathheld ^{19}F, oxygen-enhanced, and Fourier-decomposition MRI-based acquisitions.

Materials and Methods: *All Imaging was performed on a Siemens TIM Trio 3 Tesla MRI scanner, following Institutional Review Board approval.* Gas delivery is accomplished through the use of an MR compatible pneumotachometer, in conjunction with two three-way pneumatically controlled Hans Rudolph Valves. The pneumatic valves are connected to Douglas bags used as the gas source. A mouthpiece (+nose clip) or an oro-nasal Hans Rudolph disposable mask is connected following the pneumatic valve to minimize dead-space and provide an airtight seal. Continuous monitoring/sampling of inspiratory and expiratory oxygen and carbon dioxide levels at the mouthpiece/mask is achieved through the use of an Oxigraf gas analyzer.

Results: Forty-four imaging sessions were successfully monitored, during Fourier-decomposition (n = 3), fluorine-enhanced (n = 29), oxygen-enhanced, and ultra short echo (n = 12) acquisitions. The collected waveforms, facilitated proper monitoring and coaching of the subjects.

Conclusion: We demonstrate an inexpensive, off-the-shelf solution for monitoring these signals, facilitating assessments of lung function. Monitoring of respiratory efforts and exhaled gas concentrations assists in understanding the heterogeneity of lung function visualized by gas imaging.

Key Words: ventilation; fluorine-enhanced; oxygen-enhanced; respiratory gating; physiological monitoring
J. Magn. Reson. Imaging 2014;39:735–741.

THE GENERAL RELIANCE on global measurements of pulmonary function (i.e., spirometry) providing a static, albeit multiple valued, measurement of lung function has prompted the development of several MRI-based techniques to facilitate a more regional noninvasive assessment of the underlying structure and function. This reflects the inability of spirometry to provide a regional assessment of the ongoing physiological/pathological changes. In conjunction with advancements in gradient hardware and pulse sequence considerations, these MRI-based techniques such as conventional proton (^{1}H), hyperpolarized (hP) 129-xenon (^{129}Xe) (1,2), hP 3-helium (^{3}He) (3–6), 19-fluorine (^{19}F) -enhanced (7,8), oxygen-enhanced (OE) (9,10), and Fourier-decomposition (FD) (11,12), have raised interest within the pulmonary medicine arena, through noninvasive regional assessments of normal and pathological pulmonary function.

The complexity of pulmonary ventilation as a physiological process, during which gas exchange between the outside environment and internal structures occurs, is reflected in the lung's anatomic structure and localized physiologic responses. The heterogeneity of pulmonary ventilations' distribution has been shown to be dependent upon several factors including tidal volume, preinspiratory lung volume, patient positioning and gravity (13–16). To properly investigate pulmonary disease conditions using pulmonary functional MRI techniques (2,4,5,8,9,11), it is essential to provide means for proper monitoring/control of lung inflation levels and inspiratory and expiratory gas concentrations, given the heterogeneous nature of pulmonary ventilation in both normal and disease lung conditions. The strong magnetic field associated with such MRI techniques constrains the selection of devices and techniques developed for use within the multi-detector computed tomography (MDCT) and

[1]Duke Image Analysis Laboratory, Duke University School of Medicine, Durham, North Carolina, USA
[2]Department of Radiology, Duke University School of Medicine, Durham, North Carolina, USA
Contract grant sponsor: W.H. Coulter Foundation Translational Research Award.
*Address reprint requests to: H.C.C., 2424 Erwin Road, Hock Plaza Suite #301, Durham, NC, 27705. E-mail: cecil.charles@dm.duke.edu
Received January 12, 2013; Accepted April 18, 2013
DOI 10.1002/jmri.24219
View this article online at wileyonlinelibrary.com.

Table 1
^{19}F Enhanced and ^{1}H Imaging Subject Demographics and Spirometric Values

				Spirometry: absolute(%predicted)				
Gender	Age	BMI	Lung status	FVC [L]	FEV_1 [L]	FEV_1/FVC	$FEF_{25-75\%}$ [L/s]	Imaging
M	44	31.2	Normal	5.22(97)	4.12(97)	0.79(100)	3.99(103)	^{19}F & ^{1}H
M	24	24.3	Normal	6.45(116)	4.76(104)	0.74(89)	3.75(79)	^{19}F & ^{1}H
F	35	34.8	Normal	3.37(103)	2.37(87)	0.7(83)	1.64(53)	^{19}F & ^{1}H
M	18	19.4	Normal	6.2(101)	5.26(103)	0.85(100)	5.56(107)	^{19}F & ^{1}H
F	27	22.2	Normal	4.12(111)	3.59(114)	0.87(101)	4.46(123)	^{19}F & ^{1}H
F	26	22.8	Normal	3.49(94)	2.87(90)	0.82(95)	2.9(79)	^{19}F & ^{1}H
F	24	25.2	Normal	4.45(101)	3.47(92)	0.78(91)	3.04(77)	^{19}F & ^{1}H
M	35	24.6	Normal	5.22(91)	4.12(89)	0.79(98)	3.65(83)	^{19}F & ^{1}H
M	34	27.7	Normal	6.88(106)	4.46(86)	0.65(80)	2.71(88)	^{19}F & ^{1}H
M	52	38.1	Normal	4.01(89)	2.36(68)	0.59(76)	1.18(38)	^{19}F & ^{1}H
M	26	27.2	Normal	5.94(93)	4.26(92)	0.72(87)	3.18(62)	^{19}F & ^{1}H
F	51	31.0	Asthma	4.02(110)	2.91(101)	0.72(91)	2.11(76)	^{19}F & ^{1}H
F	50	32.2	Asthma/SAD	2.71(101)	2.12(99)	0.78(96)	1.89(82)	^{19}F & ^{1}H
F	30	18.8	CF/Tx	2.67(71)	2.5(78)	0.94(111)	3.92(113)	^{19}F & ^{1}H
F	30	20.8	CF/Tx	2.85(81)	2.07(69)	0.73(86)	1.56(47)	^{19}F & ^{1}H
M	29	17.8	CF/Tx	2.23(41)	1.3(29)	0.58(71)	0.95(21)	^{19}F & ^{1}H
M	67	25.2	COPD	3.48(80)	2.23(69)	0.64(86)	1.07(42)	^{19}F & ^{1}H
F	53	33.2	COPD	2.55(83)	1.53(63)	0.6(74)	0.69(28)	^{19}F & ^{1}H
M	54	30.0	COPD	5.9(105)	3.52(81)	0.6(78)	1.67(46)	^{19}F & ^{1}H
M	67	21.3	COPD	3.15(65)	0.81(22)	0.26(35)	0.22(8)	^{19}F & ^{1}H
F	51	32.7	COPD	3.85(134)	2.89(126)	0.75(92)	2.5(103)	^{19}F & ^{1}H
F	57	24.6	COPD	1.66(54)	1.28(53)	0.77(96)	1.09(45)	^{19}F & ^{1}H
M	66	27.9	COPD	3.06(88)	1.63(62)	0.53(69)	0.58(24)	^{19}F & ^{1}H
M	59	32.3	COPD	4.06(79)	2.31(59)	0.57(75)	0.73(23)	^{19}F & ^{1}H
F	71	29.9	COPD	2.98(120)	1.27(68)	0.43(56)	0.33(20)	^{19}F & ^{1}H
M	55	26.7	COPD	3.28(74)	1.95(56)	0.6(75)	0.96(29)	^{19}F & ^{1}H
F	55	23.8	COPD/Tx	3.52(106)	2.9(112)	0.82(104)	3.13(125)	^{19}F & ^{1}H
F	71	33.2	COPD/SAD	1.76(68)	1.06(54)	0.6(80)	0.37(22)	^{19}F & ^{1}H
F	56	28.9	SAD	3.57(91)	3.06(100)	0.86(109)	3.93(142)	^{19}F & ^{1}H

SAD = small airway disease; CF = cystic fibrosis; TX = lung transplant; FVC = forced vital capacity; FEV_1 = forced expiratory volume in 1 second; FEF = forced expiratory flow.

molecular imaging communities, often due to the use of ferromagnetic materials in said devices (17). Additionally, to further develop these imaging techniques as valid clinical/research tools and their appropriateness within clinical trials, it is ideal to have a single apparatus capable of performing all the desired tasks, while providing the ability to digitally record and archive the collected data. Physiorack is a modular MRI safe/conditional respiratory monitoring and gating solution, designed to facilitate proper monitoring of subjects' vital signals and their respiratory efforts, along with providing the means to gate the acquisitions based on several acquired signals. In this work, we demonstrate its applicability throughout several free-breathing and breathheld ^{19}F, OE, and FD MRI-based acquisitions.

MATERIALS AND METHODS

These studies were approved by the local Institutional Review Board, complied with HIPAA (Health Insurance Portability Accountability Act) policies and informed consent was obtained for all subjects. All imaging using oxygen and fluorine gases was carried out under INDs issued by the FDA.

Subject Population

Subjects between the ages of 18 and 71 were recruited for imaging, included nonsmoking normal subjects as well as subjects with a range of lung diseases including chronic obstructive pulmonary disease (COPD), asthma, and post lung transplantation. All subjects underwent spirometry in the standard upright position, according to the standards set forth by the American Thoracic Society (ATS). Subject demographics and spirometry are summarized in Tables 1 and 2.

Gas Delivery and Monitoring

All subjects were fitted with a mouthpiece or an oronasal disposable mask (Hans Rudolph, Shawnee, KS) and a T-valve to isolate the inspiratory and expiratory sections of the breathing circuit. Choice of mask or mouthpiece was assessed before imaging based on comfort levels and ability to perform the desired breathing maneuvers. A nose clip was used in conjunction with the mouthpieces only. Monitoring and digital archiving of respiratory waveforms throughout the duration of the imaging sessions was achieved

Table 2
OE, FD, and ^{1}H Imaging Subject Demographics and Spirometric Values

				Spirometry: absolute(%predicted)				
Gender	Age	BMI	Lung status	FVC [L]	FEV_1 [L]	FEV_1/FVC	$FEF_{25-75\%}$ [L/s]	Imaging
M	29	20.6	Normal	5.89(101)	3.89(82)	0.66(80)	2.51(53)	*OE & ^{1}H*
M	55	25.0	Normal	4.76(93)	3.77(97)	0.79(103)	3.60(108)	*OE & ^{1}H*
F	22	24.1	Normal	3.60(103)	3.14(103)	0.87(100)	4.14(113)	*OE & ^{1}H*
F	63	35.5	Normal	2.08(88)	1.59(86)	0.76(97)	1.43(79)	*OE & ^{1}H*
M	49	20.3	Normal	3.64(104)	3.33(118)	0.91(114)	5.84(197)	*OE & ^{1}H*
M	27	23.8	Normal	6.79(106)	4.65(90)	0.69(83)	3.06(60)	*OE & ^{1}H*
F	20	27.1	Normal	4.38(112)	3.48(102)	0.80(92)	3.28(86)	*OE & ^{1}H*
M	43	35.8	Normal	4.98(106)	4.13(110)	0.83(102)	4.52(130)	*OE & ^{1}H*
F	37	24.8	Normal	4.07(99)	3.06(91)	0.75(91)	2.52(74)	*OE & ^{1}H*
F	34	20.1	Asthma	3.15(74)	2.05(58)	0.65(78)	1.48(41)	*OE,^{1}H &FD*
M	27	21.7	Asthma	4.00(93)	3.61(99)	0.90(107)	4.85(118)	*OE,^{1}H &FD*
M	69	22.2	COPD	3.05(71)	2.11(67)	0.69(94)	1.34(55)	*OE,^{1}H &FD*

BMI = body mass index; FVC = forced vital capacity; FEV_1 = forced expiratory volume in 1 second; FEF = forced expiratory flow.

through the use of dual MR safe/conditional pneumotach airflow transducers (Model TSD117-MRI, Biopac Systems Inc., Goleta, CA). Inspiratory and expiratory O_2 and carbon dioxide (CO_2) gas concentrations were monitored by means of an oxygen gas analyzer, with capnography capabilities (Oxigraf O2Cap, Model 07–0193, Oxigraf Inc., Mountain View, CA). Samples of the O_2 and CO_2 levels during imaging were acquired directly at the mouthpiece or oro-nasal mask, for accurate depiction of the gaseous concentrations pre, post, and during respiratory maneuvers. Douglas bags (Harvard Apparatus, Holliston, MA) were used as the gas delivery sources following filling with the appropriate gases for the desired acquisition (25 L: ^{19}F; 100 L: 100% O_2). Switching between the gaseous agents and room air was accomplished remotely through the use of a series of Hans-Rudolph pneumatically controlled three-way valves (8600 Series). Perfluoropropane (PFP, C_3F_8; Molar Mass, 188 g/mol; Density, 8.17 g/L) mixed with 21% O_2, was the gas used during the ^{19}F-enhanced acquisitions.

Figure 1 illustrates a diagrammatic layout of the various Physiorack components and their respective locations. Each of the pneumotachometers is used separately to monitor the inspiratory and expiratory phases of the acquisitions. All components were interconnected using AFT7-L smooth bore tubing (35 i.d.) in a one-way nonrebreathing pathway, while minimizing deadspace. Oxygen saturation levels and heart rate were acquired using a finger pulse oximetry system (NONIN, Model 7500FO, Nonin Medical Inc., Plymouth, MN). To ensure subject isolation from the

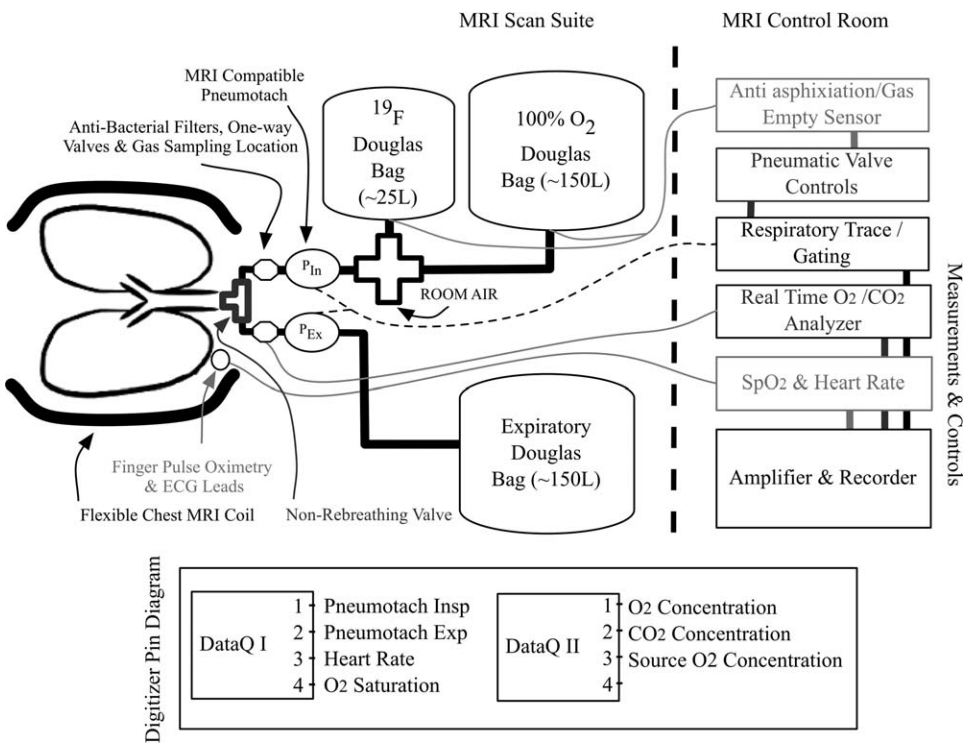

Figure 1. Diagramatic layout of Physiorack components and DataQ digital I/O pin allocations. All control units for the components used were placed inside the MR control room, while cables and gas sampling lines were passed into the MRI suite through the waveguide.

Table 3
Pulse Sequence Parameters

	GRE FLASH	3D VIBE	3D radial UTE	HASTE	trueFISP
Imaging technique	^{1}H localizers	^{19}F-enhanced	OeMRI	OeMRI	FD
Subject position	FFS	FFS	FFS	FFS	FFS
Imaging axis	Coronal	Coronal	Coronal	Coronal	Coronal
Frequency (MHz)	~123.25	~115.96	~123.25	~123.25	~123.25
Pixel (mm)	3.125x3.125	6.25x6.25	3.125x3.125	3.125x3.125	1.562x1.562
Slice (mm)	15	15	3.125	15	15
No. of slices	15–18	18	~64	1	1
Matrix	128x128	64x64	128x128	128x128	256x256
Flip angle (°)	40	70	4	171	38
Repetition time (ms)	106	13	2.54	1980	227
Echo time (ms)	2.72	1.62	0.07	15	0.99
Bandwidth (Hz/pixel)	400	130	630	651	1502

FFS = feet first supine.

breathing system, disposable filters (Vacumed, Ventura, CA) were placed inline with the breathing circuit. Furthermore, a vacuum gas sensor was placed at the Douglas bag output to serve as an anti-asphyxiation and gas-empty sensor, such that if the gas source were to be depleted during the imaging session, the resultant vacuum pressure would trigger the sensor to automatically switch the gas supply to room air. Gas sampling lines were passed through the waveguide to facilitate communication between the sensors and their respective modules in the control room. All electrical signals were reconnected by means of a radiofrequency (RF) patch panel next to the control room.

The signals recorded from the pneumotach transducers are amplified by means of transducer amplifier modules (Biopac, Model DA 100C). All sampled signals (respiratory, gaseous concentrations, pulse-oximetry, etc.) are recorded and digitized using a pair of digitizing acquisition modules (Windaq, Model DI-158, DataQ Instruments, Akron, OH). The resultant digitized signals, can then be re-routed to the manufacturers' external trigger input for use in respiratory gating. The DataQ acquisition modules are connected directly to a PC to facilitate a real-time visualization of the signals and digital archiving of the collected signals, through the use of the DataQ acquisition module software. Similarly, the O_2 and CO_2 signals are also displayed using the Oxigraf supplied software.

Imaging

Pulse sequence parameters are summarized in Table 3. Forty-four imaging sessions were performed on a Siemens TIM Trio 3 Tesla (T) MRI scanner (Siemens, Erlangen, Germany), with multi-nuclear capabilities. Conventional proton (^{1}H) localizing scans and volumetric breathheld scans, using the manufacturers' body coil and a gradient echo fast low angle shot (GRE FLASH) sequence, were acquired before the initiation of the functional scans These scans are used for localization and generation of the lung masks, respectively. ^{19}F-enhanced (using PFP) imaging (n = 29) was carried out using a three-dimensional (3D) gradient echo volume interpolated breathhold examination (GRE VIBE) sequence and a flexible vest-

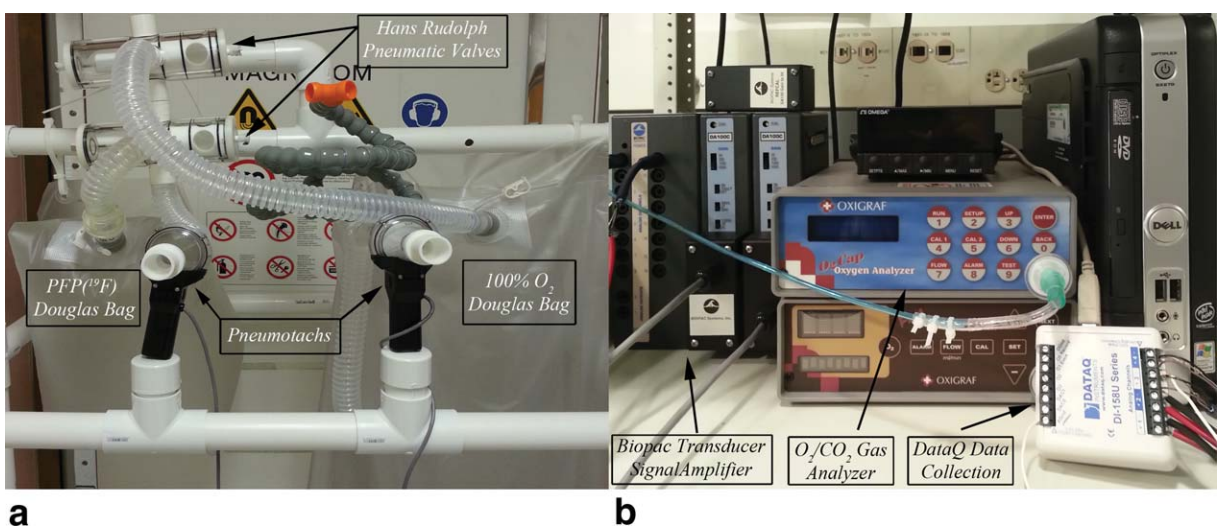

Figure 2. Actual setup of Physiorack components both inside the scanner room (**a**) and in the control room (**b**), as would be implemented during any given imaging session. (Not in picture: Oro-nasal face mask, filters and Pulse oximetry system.)

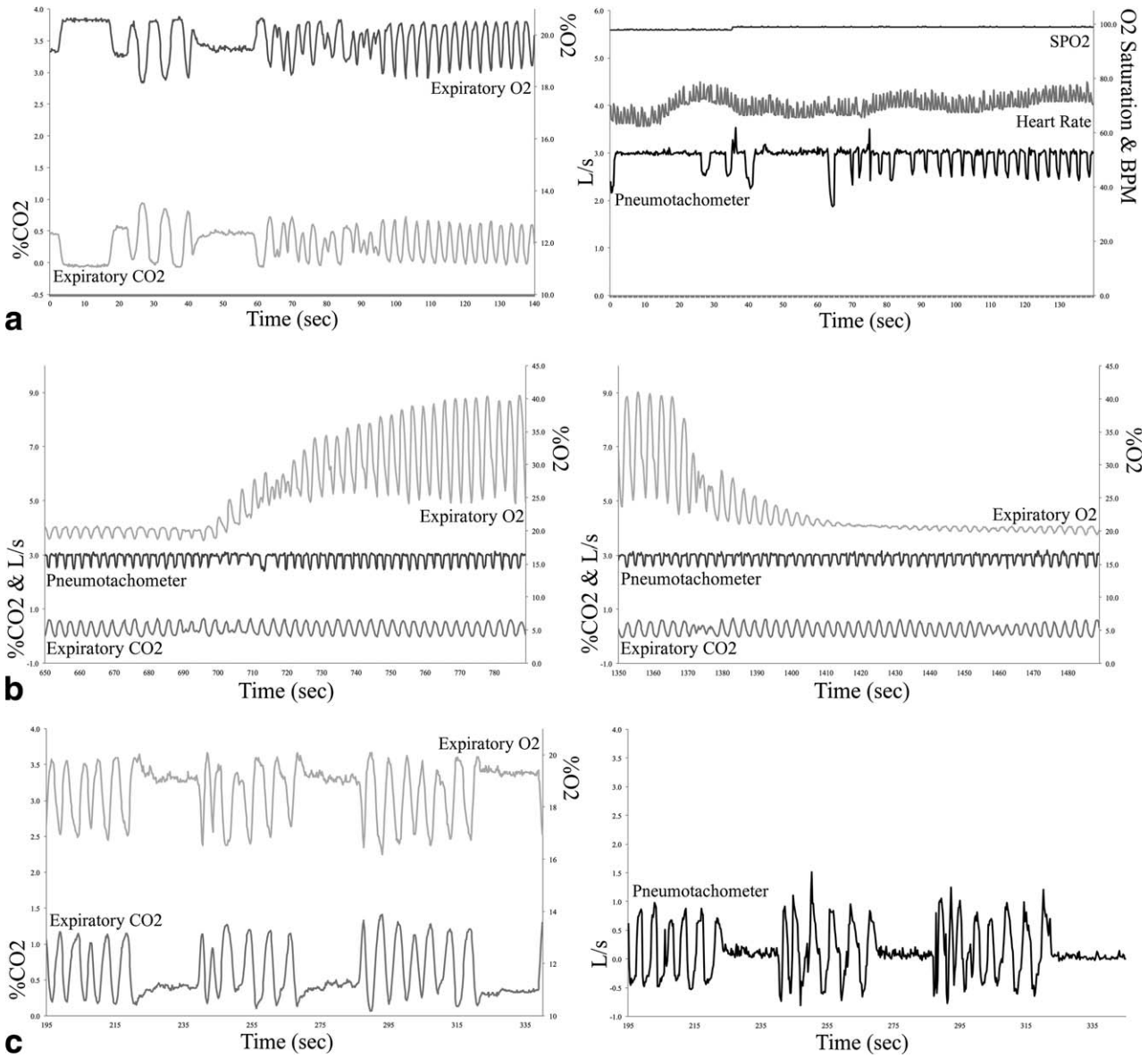

Figure 3. Sample Physiological and respiratory monitoring signals collected during end-inspiration, end-expiration and free-breathing maneuvers, demonstrate consistency of breathing maneuvers and stability during breathholds (**a**). Pneumotachometer and expired O_2 and CO_2 concentrations throughout the wash-in and wash-out of 100% O_2 during an OE imaging session facilitate proper initiation and termination of the acquisitions, while providing several suitable signals to perform respiratory gated acquisitions (**b**). Expired gaseous concentrations and pneumotachometer output during ^{19}F enhanced acquisitions, demonstrate repatability of the breathing maneuvers, accomplished through verbal ques. The ability to assess these metrics in real-time provides the means for properly assessing the exerted respiratory efforts throughout the duration of the imaging sessions (**c**).

like coil (Clinical MR Solutions, Brookfield, WI) specifically tuned to the frequency of ^{19}F (~115.9 MHz), following the inspiration of PFP. ^{19}F acquisitions included up to eight breathholds interleaved with three to five breaths of PFP, assessing the wash-in, equilibration, and wash-out phases of ventilation. OE imaging (n = 12) was performed using a 3D ultra short echo (UTE) Radial sequence with 1/2 *k*-space sampling and a 3D half Fourier acquisition single shot turbo spin echo (HASTE) sequence, each including three separate free-breathing acquisitions of 21% O_2, 100% O_2 and 21% O_2, respectively, facilitating a rough assessment of the lungs' diffusion capacity. FD imaging (n = 3) was carried out using a 2D trueFISP (fast imaging steady-state precession) sequence, throughout several 3- to 4-min free-breathing maneuvers (Siemens, Erlangen, Germany).

RESULTS

A total of 41 subjects underwent imaging using Physiorack. All respiratory maneuvers (free-breathing and breathheld) during imaging were completed without

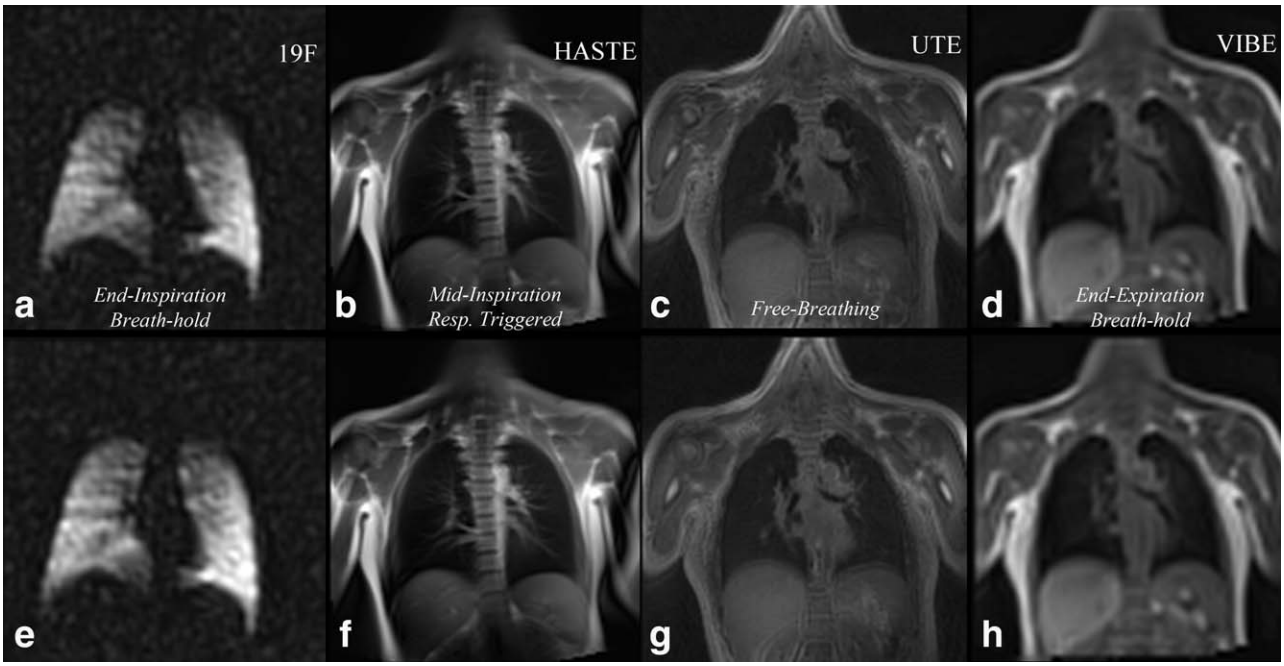

Figure 4. Repeatability of the evaluated lung field of view from PFP enhanced (**a**,**e**), conventional ^{1}H breathhold (HASTE, **b**,**f**; VIBE, **d**,**h**) and free-breathing UTE (**c**,**g**) acquisitions is demonstrated through the identical intra-technique lung coverage. HASTE, VIBE, and UTE images were all acquired from the same subject, while the PFP enhanced images are from a different subject.

any complications and/or complaints of increased resistance when gas sources were used. The median and interquartile range $\mu(25\%,75\%)$ of FEV_1 for normal (n = 20), asthma/CF (n = 8), and COPD (n = 13) subjects was 92(88,103), 88(66,99), and 63(56,69), respectively. The use of 35-mm ID tubing throughout the breathing circuit facilitated a minimal-resistance breathing environment for the subjects, specifically the elder-disease population. All collected waveforms were digitized and archived on the PC and uploaded to an in-house database. Signals acquired from Physiorack were easily visualized postimaging through the use of the DataQ supplied software or a simple spreadsheet software package. Actual setup of the majority of the Physiorack components, both inside and outside the scanner room, can be seen in Figure 2.

Respiratory gating throughout the HASTE (OeMRI) and trueFISP (FD) acquisitions was accomplished through the use of the manufacturers' internal gating software (Siemens). The ability to monitor the subjects' real-time respiratory efforts, facilitated proper verbal instruction of the subjects' to adjust their breathing patterns, such that they were approximately the same breath-to-breath.

Figure 3A illustrates sample expiratory O_2, CO_2, pneumotachometer, heart rate, and oxygen saturation recordings from a subject undergoing breathhold and free-breathing maneuvers during OE and FD imaging sessions. Stability of the end-inspiration and end-expiration breathhold maneuvers is demonstrated through the flat sections in the O_2, CO_2 and pneumotachometer recordings. Following the breathhold maneuvers, free-breathing maneuvers were initiated following relaxation of the subject's efforts to a steady-state status. Monitoring of the wash-in and wash-out of 100% O_2 before and after initiation of the OE image acquisitions is demonstrated in Figure 3B. The wash-in and wash-out periods are clearly demonstrated in conjunction with reaching steady-state breathing on either 100% O_2 or room air. In the case of the ^{19}F acquisitions, Figure 3C illustrates the expiratory O_2 and CO_2 recordings during three breathhold maneuvers interleaved with approximately five breaths of PFP and the complimentary pneumotachometer recordings during these maneuvers. The repeatability of the breathholds and subject respiratory efforts are clearly observed during the maneuvers. The ability to perform free-breathing, respiratory triggered, and breathhold imaging at different stages in the respiratory cycle and repeatability of the lung field of view between successive imaging sessions of different imaging techniques is demonstrated in Figure 4.

DISCUSSION

The apparent heterogeneity of pulmonary ventilation in normal and disease subjects has been assessed by means of hyperpolarized media (3-helium and 129-xenon) and multi-detector computed tomography, demonstrating the impact of gravity, posture, and lung volumes upon the resultant ventilation assessments. Inspiratory flow rates, tidal volume, initiating lung volumes, and posture are all factors that act variably to change the overall distribution. The underlying complexity of the pulmonary ventilation and the

factors affecting the distribution of gas and blood flow during any given maneuver must be carefully monitored during imaging for accurate assessment and differentiation between normal and abnormal physiological states and dissemination across multi-center trials.

In conclusion, the methods and results presented demonstrate the feasibility of an MRI conditional apparatus, providing physiological and respiratory monitoring of individuals undergoing free-breathing and/or breathheld imaging maneuvers through the use of 510k cleared devices. The increasing need for assessing pulmonary ventilation regionally, rather than globally by means of PFTs, has prompted the development of imaging-based methods to assess this need. The complexity of the pulmonary system gives rise to many factors affecting the overall distribution of the inspired gaseous agents, such as gravitational dependence, regional differences in lung expansion, and flow rates (15,18,19). Therefore, appropriate monitoring of flow rates, lung volumes, and respiratory efforts is needed to ensure proper assessment of the underlying structure and function, as well as suitable inter- and intra-subjects multi-modality assessments.

ACKNOWLEDGMENTS

The authors thank Samantha Womack, BA, for her efforts in subject recruitment, spirometry, and screening and Wandra Davis, RT R MR, for operation of the MRI scanner and experimental setup. We also thank Siemens Healthcare for their continuous MRI support, Air Liquide (formerly Scott Specialty Gases) for the perfluoropropane gas supply, the W.H. Coulter Foundation for their partial funding and support and the Duke Image Analysis Laboratory for its support of this project.

REFERENCES

1. Shukla Y, Wheatley A, Kirby M, et al. Hyperpolarized 129Xe magnetic resonance imaging: tolerability in healthy volunteers and subjects with pulmonary disease. Acad Radiol 2012;19:941–951.
2. Kaushik SS, Cleveland ZI, Cofer GP, et al. Diffusion-weighted hyperpolarized 129Xe MRI in healthy volunteers and subjects with chronic obstructive pulmonary disease. Magn Reson Med 2011;65:1154–1165.
3. van Beek EJ, Wild JM. Hyperpolarized 3-helium magnetic resonance imaging to probe lung function. Proc Am Thorac Soc 2005;2:528–532, 510.
4. Fain S, Schiebler ML, McCormack DG, Parraga G. Imaging of lung function using hyperpolarized helium-3 magnetic resonance imaging: review of current and emerging translational methods and applications. J Magn Reson Imaging 2010;32:1398–1408.
5. Kirby M, Svenningsen S, Owrangi A, et al. Hyperpolarized 3He and 129Xe MR imaging in healthy volunteers and patients with chronic obstructive pulmonary disease. Radiology 2012;265:600–610.
6. Diaz S, Casselbrant I, Piitulainen E, et al. Progression of emphysema in a 12-month hyperpolarized 3He-MRI study: lacunarity analysis provided a more sensitive measure than standard ADC analysis. Acad Radiol 2009;16:700–707.
7. Schreiber WG, Eberle B, Laukemper-Ostendorf S, et al. Dynamic (19)F-MRI of pulmonary ventilation using sulfur hexafluoride (SF(6)) gas. Magn Reson Med 2001;45:605–613.
8. Jacob RE, Chang YV, Choong CK, et al. 19F MR imaging of ventilation and diffusion in excised lungs. Magn Reson Med 2005;54:577–585.
9. Ohno Y, Hatabu H, Higashino T, et al. Oxygen-enhanced MR imaging: correlation with postsurgical lung function in patients with lung cancer. Radiology 2005;236:704–711.
10. Ohno Y, Hatabu H. Basics concepts and clinical applications of oxygen-enhanced MR imaging. Eur J Radiol 2007;64:320–328.
11. Bauman G, Puderbach M, Deimling M, et al. Non-contrast-enhanced perfusion and ventilation assessment of the human lung by means of fourier decomposition in proton MRI. Magn Reson Med 2009;62:656–664.
12. Bauman G, Scholz A, Rivoire J, et al. Lung ventilation- and perfusion-weighted Fourier decomposition magnetic resonance imaging: in vivo validation with hyperpolarized 3He and dynamic contrast-enhanced MRI. Magn Reson Med 2013;69:229–237.
13. Bryan AC, Bentivoglio LG, Beerel F, Macleish H, Zidulka A, Bates DV. Factors affecting regional distribution of ventilation and perfusion in the lung. J Appl Physiol 1964;19:395–402.
14. Hughes JM, Glazier JB, Maloney JE, West JB. Effect of lung volume on the distribution of pulmonary blood flow in man. Respir Physiol 1968;4:58–72.
15. Kaneko K, Milic-Emili J, Dolovich MB, Dawson A, Bates DV. Regional distribution of ventilation and perfusion as a function of body position. J Appl Physiol 1966;21:767–777.
16. Milic-Emili J. [Regional distribution of pulmonary ventilation]. Poumon Coeur 1968;24:1007–1018.
17. Fuld MK, Grout RW, Guo J, Morgan JH, Hoffman EA. Systems for lung volume standardization during static and dynamic MDCT-based quantitative assessment of pulmonary structure and function. Acad Radiol 2012;19:930–940.
18. Robertson PC, Anthonisen NR, Ross D. Effect of inspiratory flow rate on regional distribution of inspired gas. J Appl Physiol 1969;26:438–443.
19. Milic-Emili J, Henderson JA, Dolovich MB, Trop D, Kaneko K. Regional distribution of inspired gas in the lung. J Appl Physiol 1966;21:749–759.